

3D Reconstruction Using Light Field Camera

by

Kelvin Ting Wee

14954

Dissertation submitted in partial fulfillment of
the requirements for the
Bachelor of Engineering (Hons)
(Mechanical Engineering)

January 2015

Universiti Teknologi PETRONAS
32610 Bandar Seri Iskandar
Perak Darul Ridzuan

CERTIFICATION OF APPROVAL

3D Reconstruction Using Light Field Camera

by

Kelvin Ting Wee

14954

A project dissertation submitted to the
Mechanical Engineering Programme
Universiti Teknologi PETRONAS
in partial fulfilment of the requirement for the
BACHELOR OF ENGINEERING (Hons)
MECHANICAL ENGINEERING

Approved by,

(Dr. Mark Ovinis)

UNIVERSITI TEKNOLOGI PETRONAS

BANDAR SERI ISKANDAR, PERAK

January 2015

CERTIFICATION OF ORIGINALITY

This is to certify that I am responsible for the work submitted in this project, that the original work is my own except as specified in the references and acknowledgements, and that the original work contained herein have not been undertaken or done by unspecified sources or persons.

KELVIN TING WEE

ABSTRACT

3D reconstruction is important as a method to represent the real world environment using a 3D digital model. The emergence of the Lytro light field camera in the market has opened up new possibilities for researchers to explore 3D reconstruction with this easily obtained off-the-shelf product. By using depth information contained in the camera, 3D reconstruction of real life objects is made possible. However, despite its huge potential, 3D reconstruction based on light field technology is still insufficiently explored. In this work, a map is obtained by using two different responses of the image, namely defocus and correspondence response, and combining both responses to get a clearer and better depth map. In the beginning stage of research, one image with a fixed point of focus is being selected as object of study and exported in multiple file formats. Some of it contains all the light field information of Lytro image, while others contain selective information such as depth data or representation of 2D image. At the initial stage, a preliminary depth map was obtained but the depth representation was not clear and obvious. In the end a 3D depth map that has the outline and shape of a real object studied was generated. It was later found out that defocus analysis can be improved by reducing the defocus analysis radius. All in all, a 3D depth map can be successfully obtained from light field picture through computations in MATLAB code.

ACKNOWLEDGEMENT

I would like to extend my sincere gratitude to my supervisor Dr. Mark Ovinis who has given me encouragements, advices, opinions in completion of this project. With his help and encouragement in many stages of this project, I am able to carry out this project smoothly.

Furthermore, I would also like to acknowledge with much appreciation the guidance of a Phd student, Osman. At the beginning stage of my project, he gave a lot of useful advices and suggestions as well as a thorough introduction of the project. His patience in guiding and teaching helped me a lot in kick-starting the project.

Besides, I am grateful to some of the panels as some recommendations given by them during the project presentation has improved my presentation skills and they also gave me advices on the future recommendations for the project.

Last but not least, I would also like to take this opportunity to express my sincere thanks towards my family and friends who are always there to encourage me and give me support. Their support is one of the reasons which keeps me going throughout the highs and lows of this project.

TABLE OF CONTENTS

CERTIFICATION OF APPROVAL	i
CERTIFICATION OF ORIGINALITY	ii
ABSTRACT	iii
ACKNOWLEDGEMENT	iv
CHAPTER 1:	INTRODUCTION	1
	1.1. Background	1
	1.2. Problem Statement	3
	1.3. Objective and Scope of Study.	3
CHAPTER 2:	LITERATURE REVIEW	4
	2.1 Multi-Image 3D Reconstruction	4
	2.2 3D Reconstruction from Multi-Focused Images	4
	2.3 3D Reconstruction by Modifying Cameras	5
	2.4 3D Reconstruction by Combining Responses	5
CHAPTER 3:	METHODOLOGY	7
	3.1. Research Methodology	7
	3.2 Key Milestones	8
	3.3 Gantt Chart	9
	3.3.1 FYP I	9
	3.3.2 FYP II	10
CHAPTER 4:	RESULTS AND DISCUSSIONS	11
	4.1 Generating 2D Depth Map	11
	4.2 Decoding and Visualising Planar Slices	12
	4.3 Compute Defocus and Correspondence Responses	13
	4.4 Defocus and Correspondence Responses	16
	4.5 Generating 3D Depth Map	17

4.6	Manipulating Defocus and Correspondence Radius	20
CHAPTER 5:	CONCLUSION AND RECOMMENDATION	. 26
5.1	Conclusion 26
5.2	Recommendation 27
REFERENCES	28

LIST OF FIGURES

Figure 1.1: Lytro (1st version)	2
Figure 1.2: Lytro Illum (2 nd version)	2
Figure 4.1: Image of Study	9
Figure 4.2: Comparison of Real Image (Left) and 2D Depth Map (Right)	10
Figure 4.3: Output from LFT/slicer	11
Figure 4.4: Successful Workflow of “Tao13_LF_Depth” MATLAB Code	12
Figure 4.5: Input Data (Picture of a Plant)	13
Figure 4.6: Image Set (Result) – Defocus Analysis (Left), Correspondence Analysis (Middle), Final Depth Estimations (Right)	14
Figure 4.7: Range of Z Coordinates from 3D Depth Map (Side View)	15
Figure 4.8: Depth Map (362 x 311)	16
Figure 4.9: 3D Depth Map (Top View)	19
Figure 4.10: 3D Depth Map (Bottom View)	19
Figure 4.11: 3D Depth Map (Left), Input Picture (Middle), Superimposition (Right)	20
Figure 4.12: Own Data from Lytro Camera	19
Figure 4.13: Sheared Picture of Own Data	19
Figure 4.14: Resulting Image Set of Own Data– Defocus Analysis (Left), Correspondence Analysis (Middle), Final Depth Estimations (Right)	20
Figure 4.15: Image Set (Result with Defocus Analysis Radius = 1) – Defocus Analysis (Left), Correspondence Analysis (Middle), Final Depth Estimations (Right)	20
Figure 4.16: Correspondence Analysis Result – Radius = 1(Left), Radius = 9 (Middle), Radius = 20 (Right)	21

LIST OF TABLES

Table 4.1: Effect of Change in Defocus Radius on Analysis Result	22
Table 4.2: Effect of Change in Correspondence Radius on Analysis Result	23

CHAPTER 1

INTRODUCTION

1.1 BACKGROUND

3D reconstruction is a process that aims to produce a 3D digital model as its end product. The 3D digital model produced is able to represent a real world environment in terms of its shape, appearance and dimensions [1]. 3D digital models can be useful for applications such as reverse engineering, quality control or metrology inspection, industrial design, entertainment industry, or even documentation of cultural artefacts. The ability to obtain 3D digital models effectively and accurately can save time and effort if compared to measurements by hand or tools.

Few methods are available for 3D reconstruction, such as using a laser range finder (LiDAR), a Kinect camera, or a time-of-flight terrestrial 3D range scanner [2]. A laser range finder produces high density and high quality depth data, but often requires complicated and extensive algorithms to process the data to be useful for 3D reconstruction [1]. In certain cases, modifications of camera had to be done, such as masking the aperture and modifying the lenses, besides the hassle of modifying the camera, masking the aperture would reduce the amount light captured by the camera. Other professional 3D reconstruction equipment such as a time-of-flight terrestrial 3D range scanner promises good results, but are very expensive and inflexible, therefore, only applicable in certain situations such as doing a 3D reconstruction for a building where there is an open space with flat ground. A Kinect camera on the other hand, is a low cost commercially available equipment that can provide useful depth data, but has low resolution and is limited to indoor applications.

A Kinect camera is a commercial low cost equipment that can provide useful depth data, but has low resolution and is limited to indoor applications. A light-field camera (also known as plenoptic camera) captures information about the intensity of light in a scene, and also captures information about the direction that the light rays

are traveling in space. The commercial availability of light field cameras such as Lytro and Raytrix opens up new possibilities for 3D reconstruction, which might be potentially better than most of the 3D reconstruction methods available today. The light field camera used in this project is the 1st version Lytro light field camera.



Figure 1.1: Lytro (1st version)



Figure 1.2: Lytro Illum (2nd version)

One of the advantages of a light field camera in 3D reconstruction is that it allows the data acquisition process to be much easier. This is because capturing extra information about a scene is possible due to a different type of lens design compared to conventional cameras [3]. The extra information captured using a Lytro light-field camera includes depth data and directions of the incident light at the particular moment when the photo was taken, which can be utilised to refocus the image retrospectively. For 3D reconstruction, the depth data that can be obtained is of interest [4].

Depth data normally consist of a cloud of 3D coordinates, which is more commonly referred as point clouds, that depicts the dimensions and shapes of real world objects and environment. These 3D coordinates are essential in constructing a successful 3D digital model.

The aim of this project is to utilise the technology of a light-field camera to construct a 3D digital model of the real world environment.

1.2 PROBLEM STATEMENT

The accuracy of the 3D model reconstructed based on light field technology is low despite its huge potential.

1.3 OBJECTIVE AND SCOPE OF STUDY

3.1 Objective

To improve the accuracy of a 3D model reconstructed based on light-field camera by optimising the image processing steps

3.2 Scope of Study

- (i) 3D reconstruction of stationary objects as 3D reconstruction of moving objects is more complex and time consuming. Furthermore, the image acquisition process e.g. lighting variation, camera placement, etc will not be investigated

CHAPTER 2

LITERATURE REVIEW

2.1 Multi-Image 3D Reconstruction

One of the methods for 3D reconstruction is multi-image 3D reconstruction. This method involves using a normal high resolution camera (DSLR) to capture multiple images of a large building from different angles and position, and then processing the images separately and finally combining the information together using Agisoft PhotoScan SFM-DMVR software to achieve 3D reconstruction [2]. The major disadvantage of this approach is that it is computationally expensive. It would require more than 20 hours to build the satisfactory 3D digital model with an 8-core Intel i7 processor at 3.50 Ghz, 32GB of RAM and a NVidia Geforce GTX580 3GB RAM graphics card [2].

2.2 3D Reconstruction from Multi-Focused Images

The University of Calabria, Italy presented a method of 3D reconstruction of small sized objects from a sequence of multi-focused images [5]. For this method, controlled lighting and a specially calibrated stage is required. In this controlled environment, multi-focused images of different parts of a small object mounted on the stage will be captured using a high resolution conventional camera. These photos will then be processed using Multi-View Stereo Software PMVS2 for 3D reconstruction of the small object. The main disadvantage of this method is that it requires a controlled environment, which is often not the case for outdoor 3D reconstruction purposes. Besides that, this method is only applicable for reconstructing 3D model of small objects.

2.3 3D Reconstruction by Modifying Cameras

There had been efforts to modify conventional cameras so it uses the principle of light field to achieve 3D reconstruction [6]. One of these methods is to mask the aperture of a high resolution conventional camera to make it an external mask based depth and light field camera [6]. This will result in only allowing light rays within small field of view to enter the aperture of camera. Through the known properties of the mask, the angular information can be captured and studied. Multi depth fusion and Markov Random Field (MRF) is used to process the information and produce a depth map. However, the masking will result in less light entering the aperture of the camera, which might be a problem in low light conditions.

2.4 3D Reconstruction by Combining Responses

An alternative is to obtain depth from combining defocus and correspondence using light-field cameras. The basic steps of this method is to analyse 2D epipolar image obtained from light-field camera images, obtain the defocus and correspondence depth of the images, and lastly combine the information and use MRF to obtain depth information to be constructed to a 3D digital model [7]. The combined depth results in a better representation but the results are not consistent. The combined results can also be easily affected by dark and bright features of object. To overcome this, a certain calibration or manipulation in the algorithm can be done to adapt the usage of this method to different light field pictures under different conditions. Specifically the correspondence and defocus radiuses can be investigated to improve the depth representation results.

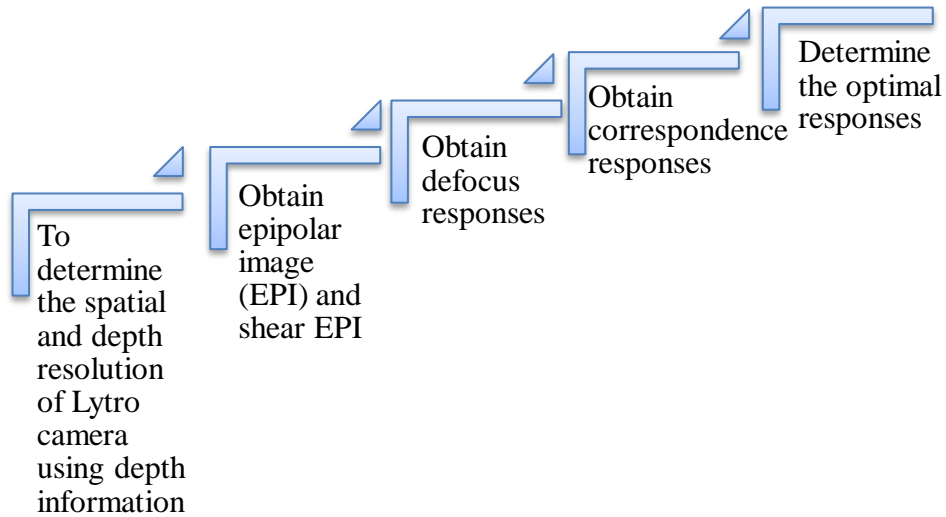
To use a light-field camera for 3D reconstruction, it uses the general and distinct steps for any 3D reconstruction, data acquisition, manipulation and application [8]. Using a light-field camera for 3D reconstruction is possible because the data acquired includes depth data, which can be obtained from depth of field. In a photo taken by a light-field camera, depth of field is actually a range where the image is focused, beyond that depth of field, the image will be defocused [9]. The depth data will then be manipulated through defocusing and correspondence to

obtain 3D coordinates to form 3D data. These manipulated data can later be prepared to go through 3D data management processes to achieve 3D reconstruction that can be useful for various industrial applications. In short, the 3D reconstruction in this project goes through three main and distinct steps, firstly is to capture an image using Lytro, and extract the depth map or depth information from the photo, and process the information to do 3D reconstruction.

CHAPTER 3

METHODOLOGY

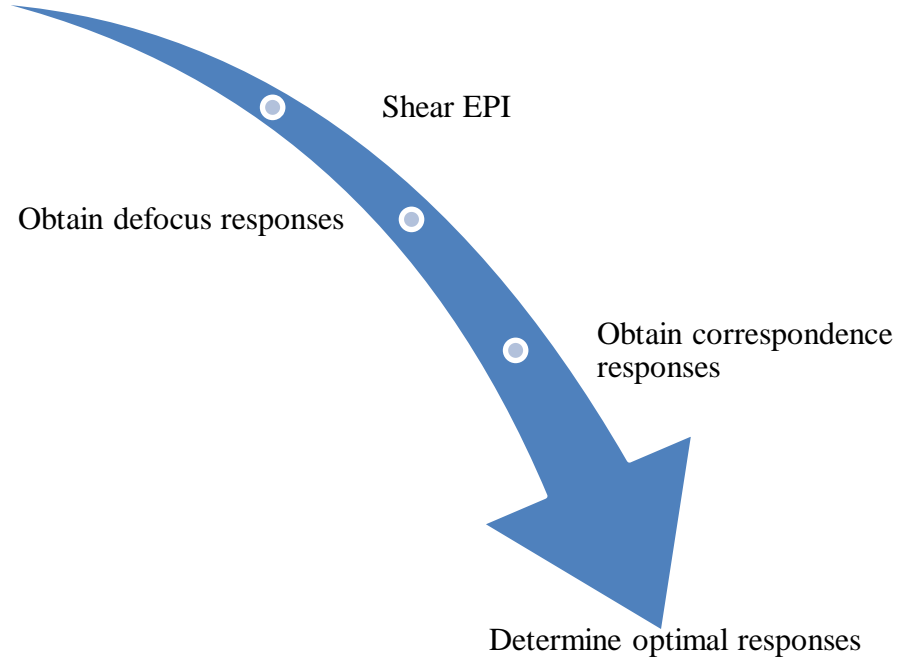
3.1 RESEARCH METHODOLOGY



The first step in the research methodology is to determine the spatial and depth resolution of Lytro camera. This is important as the resolutions will later be used as parameters for inputs of the algorithm. To obtain epipolar image (EPI) and shear the EPI is basically to cut the image into tiny segments, the purpose of this is to prepare it for the data processing step. To compute defocus responses is basically to compute the horizontal variance after vertical integration, to compute the correspondence responses is to compute the angular variance [7]. Lastly the responses will go through a Markov Random Field optimization process.

3.2 KEY MILESTONES

Determine spatial and depth resolution



3.3 GANTT CHART

3.3.1 FYPI

Project Activities	Date:	22/9	29/9	06/10	13/10	20/10	27/10	03/11	10/11	17/11	24/11	01/12	08/12	15/12	22/12	
	Week:	1	2	3	4	5	6	7	8	9	10	11	12	13	14	
Analyze researches about project	Process															
Obtain images under controlled environment and identify image for the purpose of study						Process										
Set a fixed point of focus (foreground in this period of study) and export data in various formats: .lfr, .tiff, .png etc.								Process								
Run MATLAB Codes for Lytro Images									Process							
Analyse the results of MATLAB Codes												Process				
Determine spatial and depth resolution of Lytro camera														Process		

 Process

 Key Milestone

3.3.2 FYP II

Project Activities	Date:	22/9	29/9	06/10	13/10	20/10	27/10	03/11	10/11	17/11	24/11	01/12	08/12	15/12	22/12
	Week:	1	2	3	4	5	6	7	8	9	10	11	12	13	14
Obtain epipolar image (EPI) and shear EPI	Process		Key Milestone												
Obtain defocus responses using MATLAB				Process			Key Milestone								
Obtain correspondence responses using MATLAB							Process			Key Milestone					
Determine the optimal responses using MATLAB										Process			Key Milestone		
Document all results and prepare for presentation												Process			Key Milestone

 Process
  Key Milestone

CHAPTER 4

RESULTS AND DISCUSSION

4.1 Generating 2D Depth Map

Image with clear 3D characteristics was used in this study. The focus point of the image is fixed to one point in the picture to fully study the effects of the manipulating variables to the object.

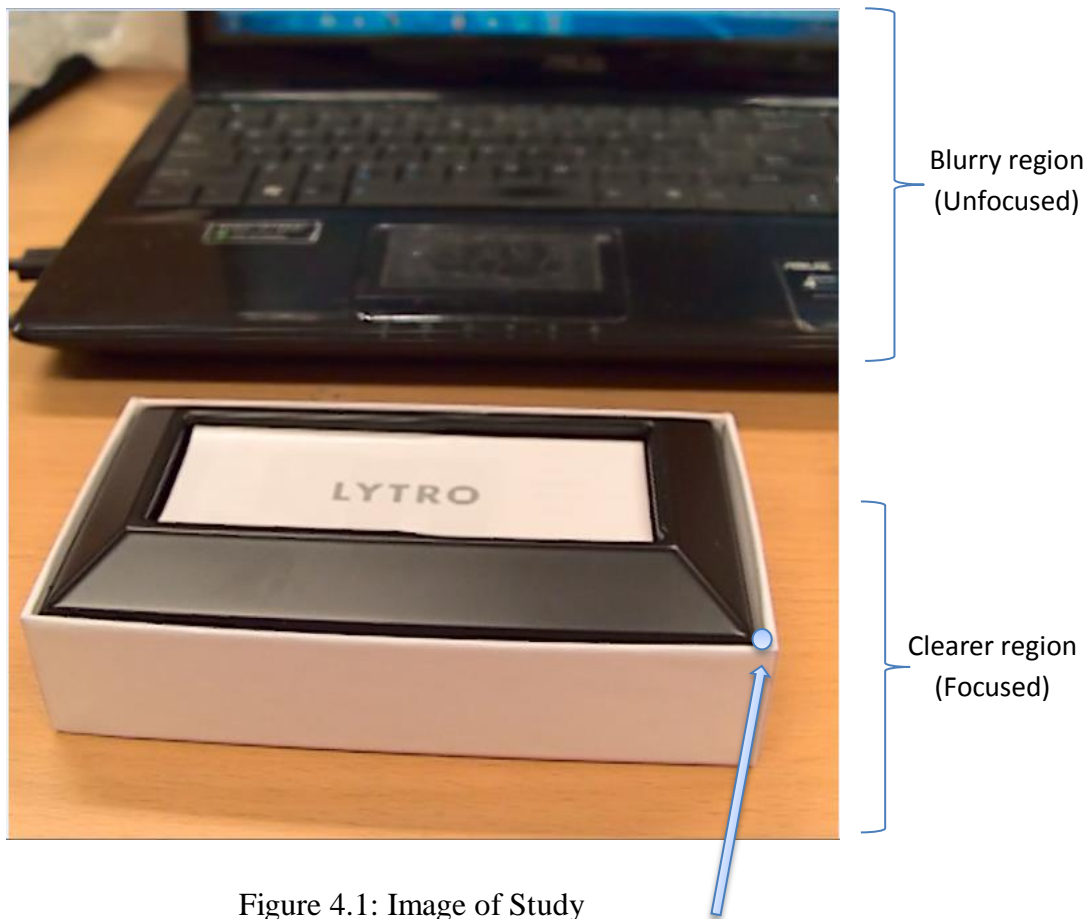


Figure 4.1: Image of Study

Image is focused at this point

A depth image was successfully obtained from the image of study, the image represents the real world using the intensity of colour. A higher intensity or a darker grey colour in the depth image represents a distance that is nearer to camera or the foreground of the image. A low intensity or light grey colour in the preliminary depth

image indicates object that is further away from camera, or at the background of the image. In short, the higher the intensity of colour in the depth image, the nearer the object is to the camera or to the foreground and vice versa. Although a depth image was successfully obtained as shown in Figure 4.2 (right), the depth is not obvious and clear from the figure pictures. More complicated codes have to be implemented on the pictures to obtain a more detailed depth image that has better quality.

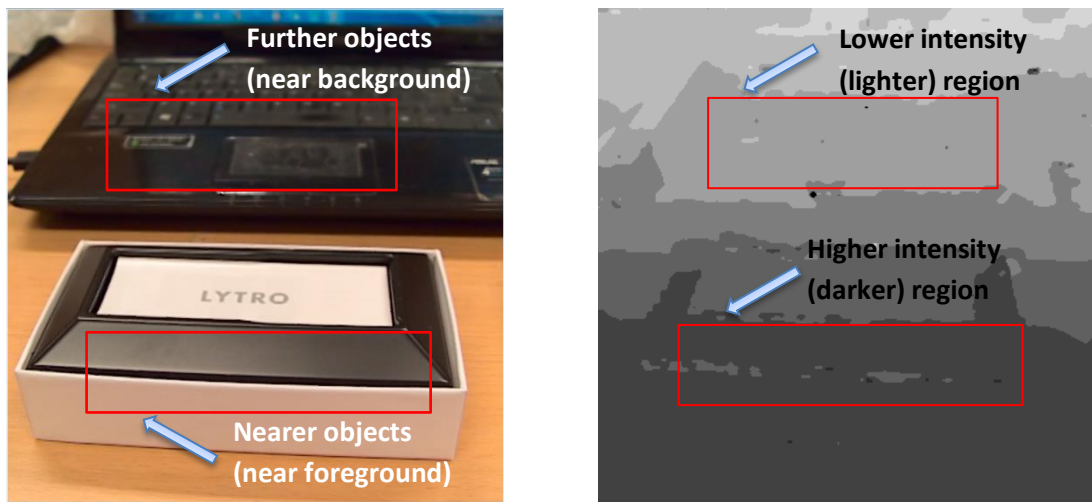


Figure 4.2: Comparison of Real Image (Left) and 2D Depth Map (Right)

4.2 Decoding and Visualising Planar Slices

Two sets of MATLAB code had been tested to generate 3D data. The first is the “LFTtoolbox0.3”, and the second is the “slicer_2013.11.28”. LFTtoolbox0.3 is a set of tools for working with light field (plenoptic) image in MATLAB. Its features include decoding, camera calibration, rectification, colour correction and visualization of light field images. “LFTtoolbox0.3” has functions for reading gantry-style light fields and for directly reading Lytro LFP files including support for Lytro Illum and Lytro Desktop 4. On the other hand, “slicer_2013.11.28” consists of interfaces for exploring 3D images by visualizing planar slices. The interface also allows displaying 3 orthogonal slices, either in 3D or in three subplots.

Testing had been done on the MATLAB codes, but no useful result have been obtained yet, in most cases there are errors in running the code, possibly because of incompatibility of input data or missing inputs.. The MATLAB codes have to continue to be explored and tested. The result of the MATLAB codes is shown in Figure 4.3.

The spatial resolution of Lytro camera is 380 x 380 pixels. Its depth resolution has yet to be determined. At present, the 3D data can only be visualised as a depth map, but the depth information cannot be extracted yet. Depth resolution depends on the type of camera or equipment used and also the performance of that particular equipment.

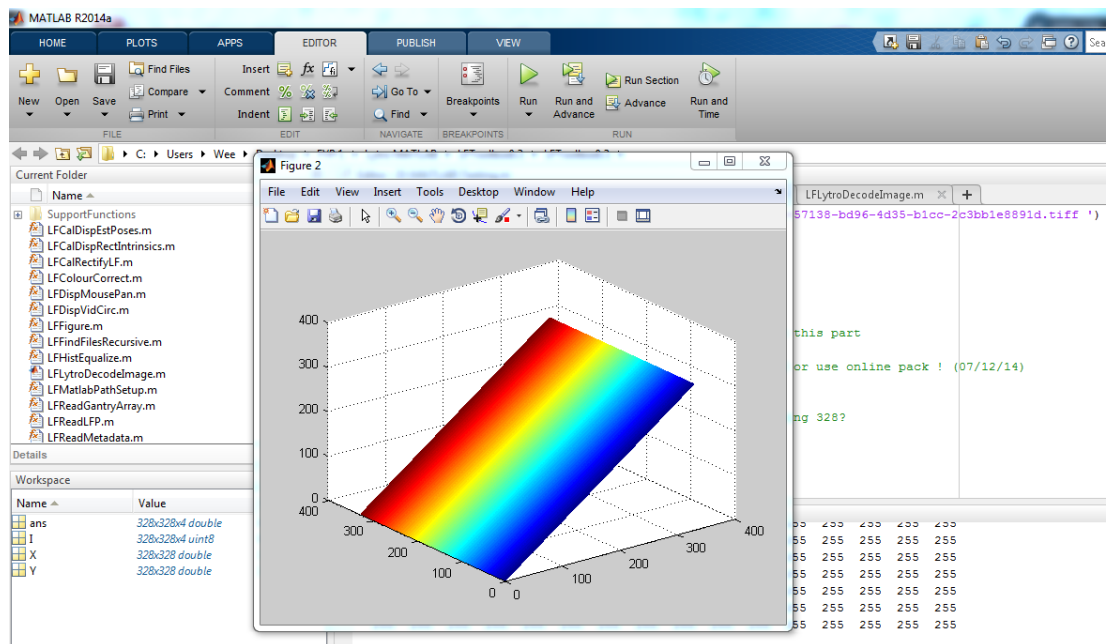


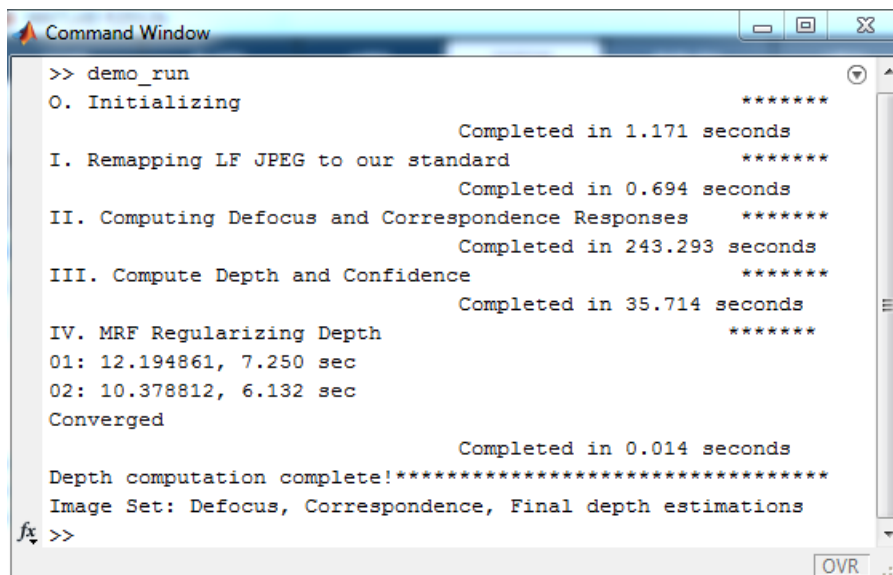
Figure 4.3: Output from LFT/slicer

4.3 Compute Defocus and Correspondence Responses

Since previous attempts of using “LFTtoolbox0.3” and “slicer_2013.11.28” failed in generating a reasonable depth map, a new MATLAB code “Tao13_LF_Depth” is being tested [7]. “Tao13_LF_Depth” is an algorithm that acts as a principled algorithm that computes dense depth estimation by combining both

defocus and correspondence depth cues. Defocus cues are previously obtained through multiple image exposures focused at different depths, while correspondence cues needs multiple exposures at different viewpoints or multiple cameras, now both of the cues can be obtained in a single capture using a light field camera.

The algorithm was tested successfully and results were generated using the sample data [7]. Figure 4.4 shows the successful work flow of the algorithm tested and the time it consumed. The code works in 4 stages, the first stage is to remap the light field jpeg file to a standard compatible with the algorithm. The second stage is to shear the EPI and compute both defocus and correspondence and depth cue responses. The third stage involves finding the optimal depth and confidence of the responses, this is done by choosing the highest response for defocus responses and lowest response for correspondence responses using mathematical formulas inputted into MATLAB. Lastly both cues are combined in a Markov Random Field (MRF) global optimization process in the fourth stage [10]. The depth resolution is set to be a default value of 256 [7].



```
>> demo_run
0. Initializing *****
                               Completed in 1.171 seconds
I. Remapping LF JPEG to our standard *****
                               Completed in 0.694 seconds
II. Computing Defocus and Correspondence Responses *****
                               Completed in 243.293 seconds
III. Compute Depth and Confidence *****
                               Completed in 35.714 seconds
IV. MRF Regularizing Depth *****
01: 12.194861, 7.250 sec
02: 10.378812, 6.132 sec
Converged
                               Completed in 0.014 seconds
Depth computation complete!*****
Image Set: Defocus, Correspondence, Final depth estimations
fx >>
```

Figure 4.4: Successful Workflow of “Tao13_LF_Depth” MATLAB Code

As shown in the MATLAB command window of Figure 4.4, most of the time of computing was in the second stage: “Computing Defocus and Correspondence Responses”. This is because in the second stage the determination of spatial gradient for defocus responses and angular variance for correspondence responses is computationally intensive. Figure 4.5 shows the sample input data while Figure 4.6 shows the results generated in the form of image set.

As shown in the image set in Figure 4.6, by comparing the left image (result from defocus analysis) and the middle image (result from correspondence analysis), it can be clearly seen that the middle image has a better and clearer representation of the plant outline in the foreground but have noisy data in the background (scattering dots in the background) that can affect the accuracy of 3D map, while the left image has a clearer representation of the background (clearer background with less noisy data) but a poor representation of the outline of the plant in the foreground. Therefore by combining both of the analysis and using MRF optimization code, a clearer and better depth image can be produced.



Figure 4.5: Input Data (Picture of a Plant)

4.4 Defocus and Correspondence Responses

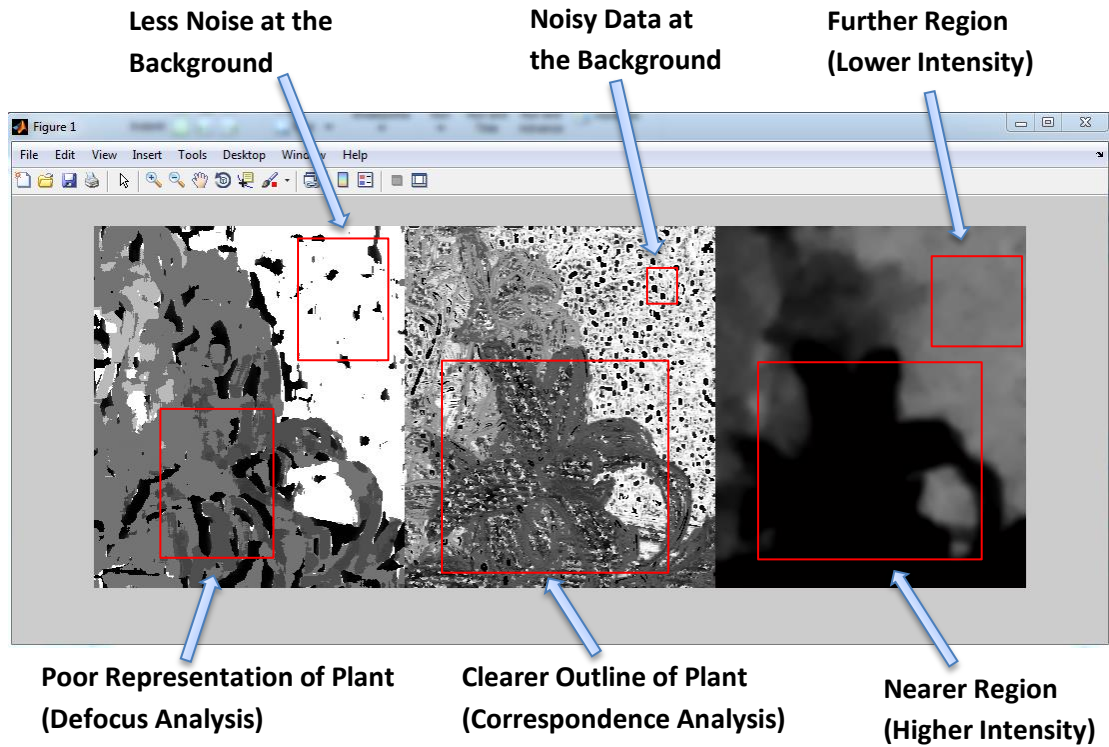


Figure 4.6: Image Set (Result) – Defocus Analysis (Left), Correspondence Analysis (Middle), Final Depth Estimations (Right)

A depth output in table form is also obtained. The depth output is in 362×311 matrix, as shown in Figure 4.13. The depth ranges from -0.1298 to 0.5329. 362×311 represents the X and Y coordinates of the depth map, while the value that ranges from -0.1298 to 0.5329 represents the Z coordinates. Z coordinate indicates the depth at different points of the represented depth map, values nearer to 0 represents nearer objects with respect to the camera. On the other hand, the larger the value of Z coordinate, the further the object is from the camera when the picture was captured. The reason for the small values for Z coordinate is because the actual depth information is being scaled down. To obtain the actual depth values, certain calibrations might be needed, examples of calibrations methods available includes checkerboard calibration, plane based calibration, and also joint depth and colour calibration.

4.5 Generating 3D Depth Map

The 3D depth map generated is shown in Figure 4.7, 4.8, 4.9, and 4.10. For the depth map that is represented in RGB (Red, Green, Blue), blue colour represents near objects with respect to the camera, green colour represents objects with medium distance, and red colour represents objects that are farthest from the camera, as shown in Figure 4.11.

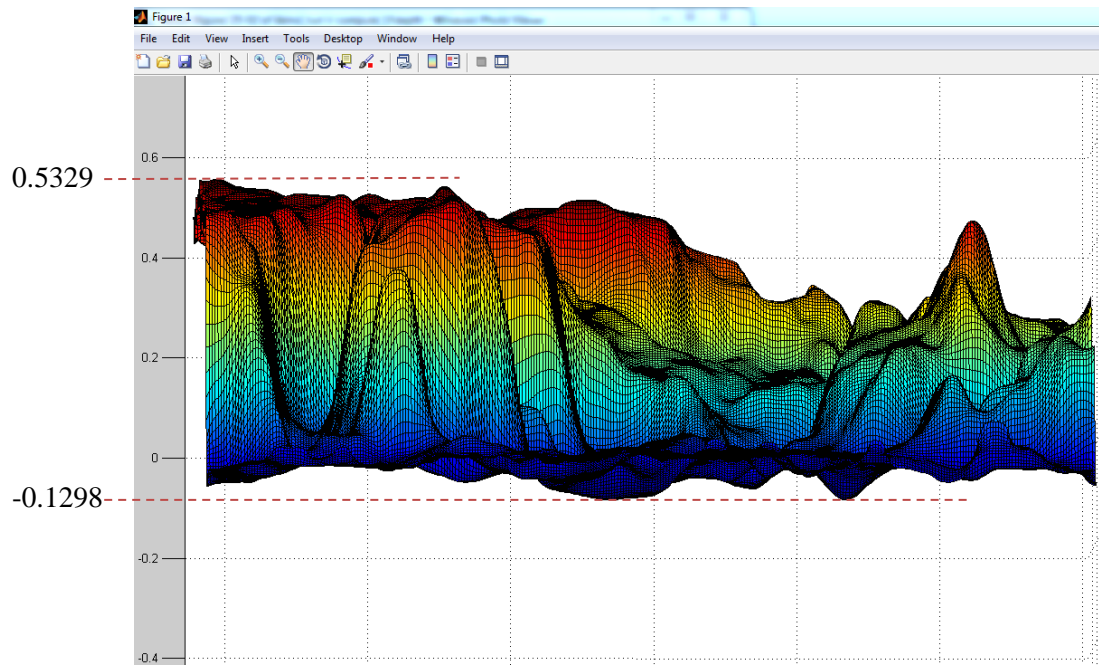


Figure 4.7: Range of Z Coordinates from 3D Depth Map (Side View)

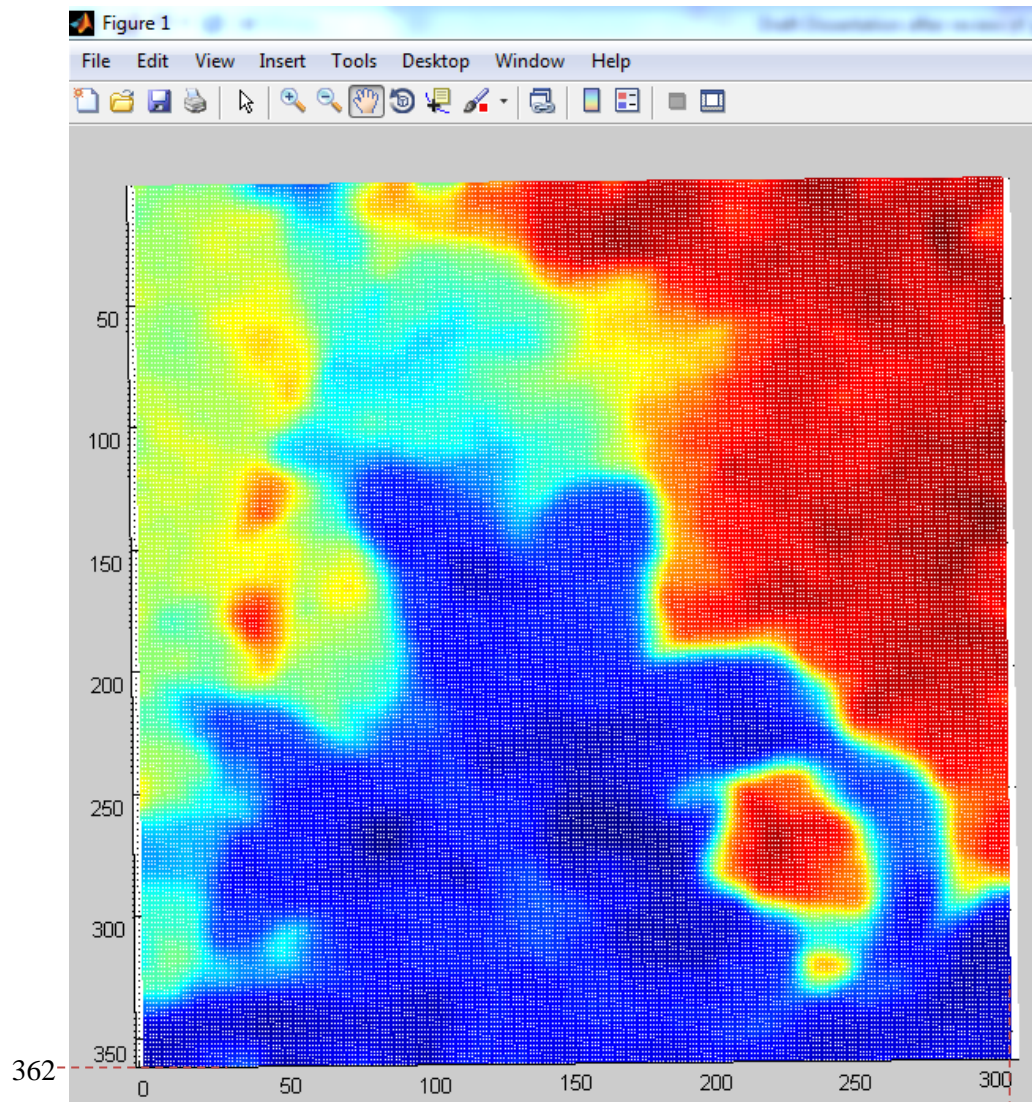


Figure 4.8: Depth Map (362 x 311)

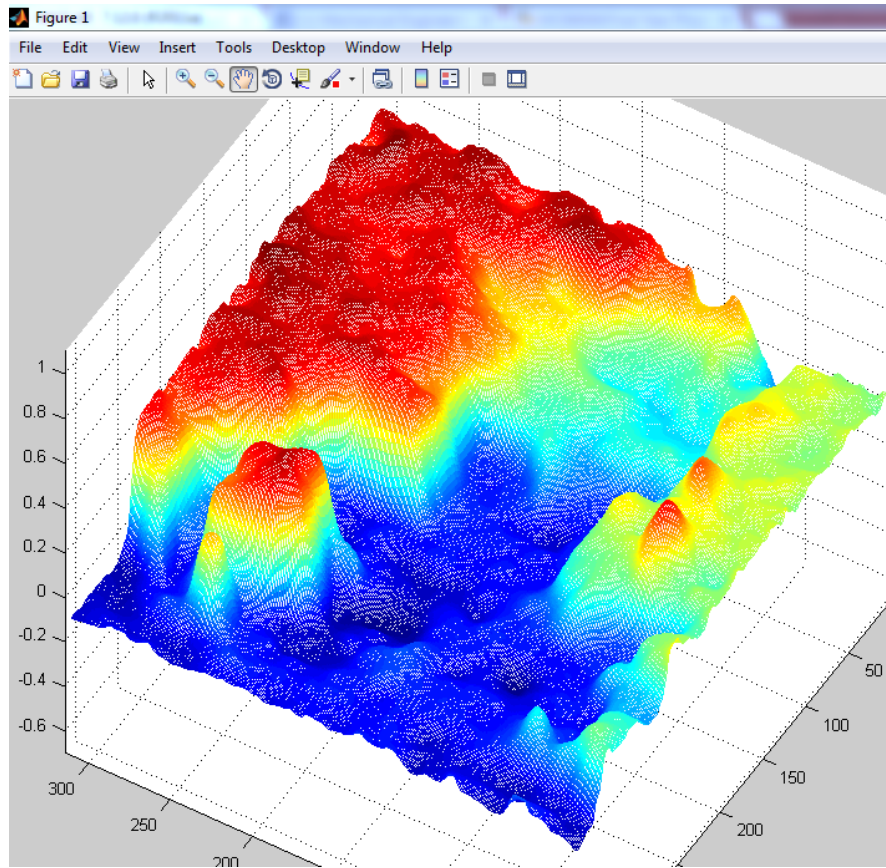


Figure 4.9: 3D Depth Map (Top View)

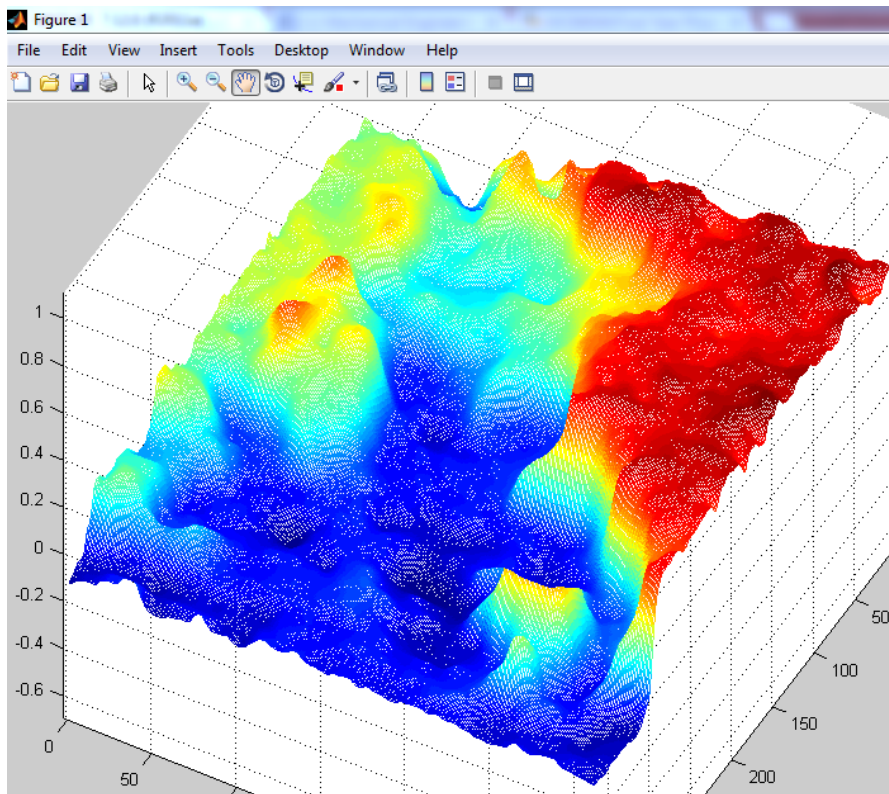


Figure 4.10: 3D Depth Map (Bottom View)

By having a comparison between the 3D depth map produced and the real picture as shown in Figure 4.11, it can be seen that up till this stage, a relatively accurate 3D depth map can be acquired. This is shown by the outlines of the plant that are identical in the 3D depth map and real picture, with correct representation of the plant that is nearer to the camera (blue region) and other plants or trees that are further from the camera (red, yellow and green region).

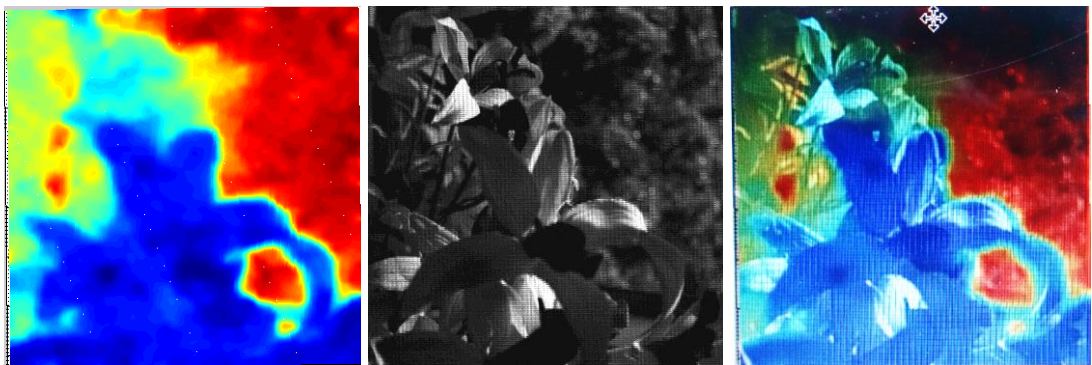


Figure 4.11: 3D Depth Map (left), Input Picture (Middle), Superimposition (Right)

4.6 Manipulating Defocus and Correspondence Radius

Attempts to generate similar results using user data from Lytro camera have failed with errors at the computation stage, suspected to be due to a difference in input file format and content of the input file [11]. The computation failed in the stage of shearing the EPI. With some minor modifications in the MATLAB code and using “Cygwin” terminal to compile “lftools” package, similar results using own data can be obtained. Figure 4.12 shows the picture obtained from Lytro camera, where a Tupperware bottle is the focus of the image, while Figure 4.13 shows the sheared picture after successful modifications in MATLAB code and compilation of packages. The generated result is shown in Figure 4.14.

The effect of shearing as shown in Figure 4.13 is the division of the original picture to a picture with multiple segments or pixels. This is to prepare the image to undergo defocus and correspondence analysis. In Figure 4.14, the generated result

shows the correspondence analysis (middle) successfully shows the features of the bottle in the picture while the defocus analysis (left) yields a result that has no clear distinction on features of the bottle, as well as blurry outlines of objects that are mixed together.



Figure 4.12: Own Data from Lytro Camera

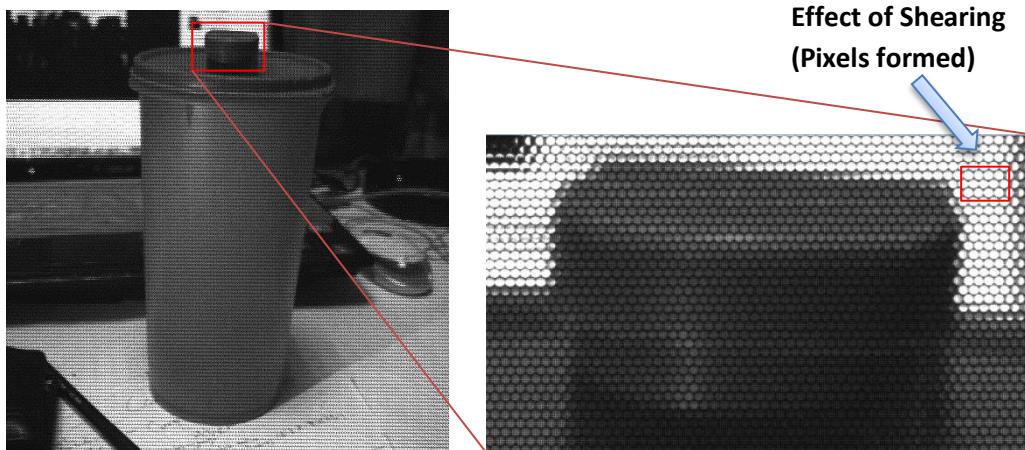


Figure 4.13: Sheared Picture of Own Data

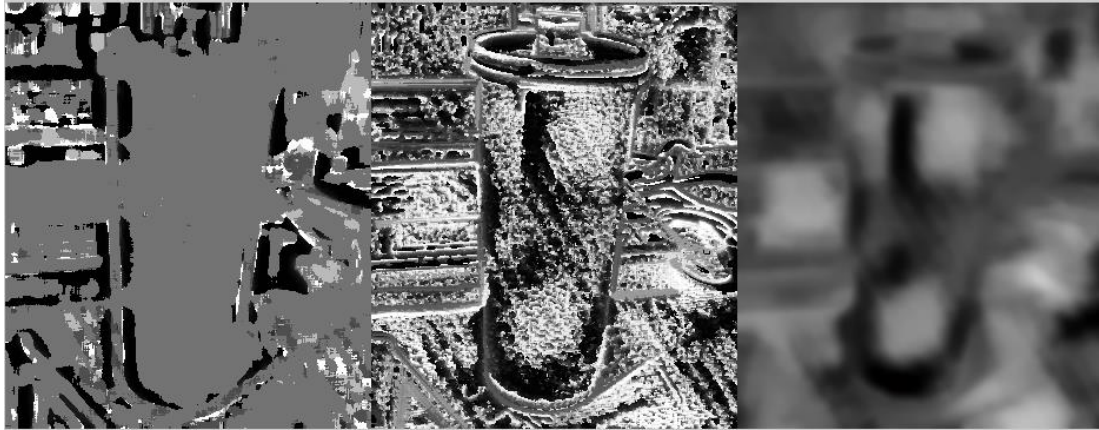


Figure 4.14: Resulting Image Set of Own Data– Defocus Analysis (Left), Correspondence Analysis (Middle), Final Depth Estimations (Right)

In order to obtain a better defocus analysis, the parameter value of the defocus analysis radius in the Tao13_LF_Depth algorithm was changed. Defocus analysis radius determines the radius or area of each computation of defocus analysis that will be performed in a particular image. Theoretically, the smaller the defocus analysis radius, the clearer the distinction of the depth image will be. The defocus analysis radius is varied from a value of 9 to 1. As a result, defocus result in Figure 4.15 depicts a successful distinction of features of the bottle and surrounding objects if compared to defocus result in Figure 4.14 with a defocus analysis radius of 1.

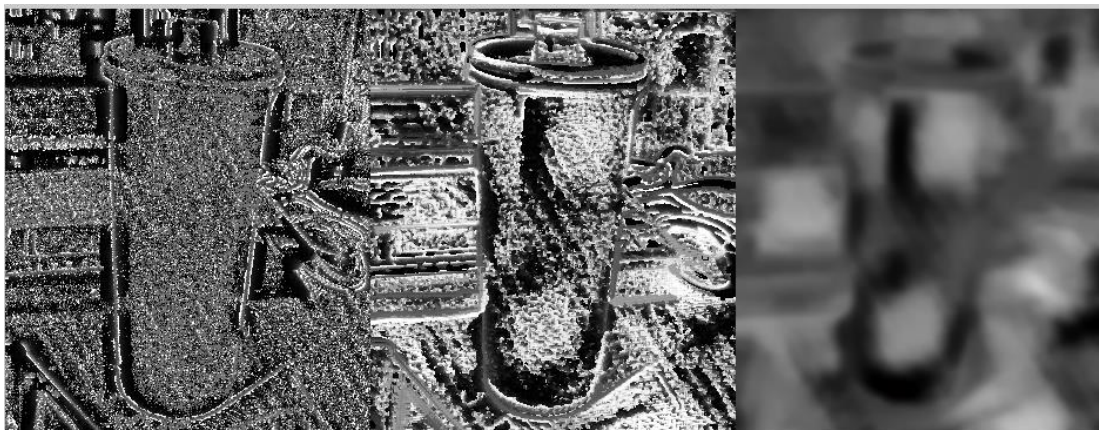


Figure 4.15: Image Set (Result With Defocus Analysis Radius = 1) – Defocus Analysis (Left), Correspondence Analysis (Middle), Final Depth Estimations (Right)

To investigate the effect of correspondence analysis radius, the radius is both decreased and increased from its default value of 9. From Figure 4.16 it can be seen that when correspondence analysis radius is decreased to a value to 1, the distinctive features of the objects start to become less obvious, and many noisy data are present in the analysis. This will cause the 3D reconstruction be less accurate. On the other hand, as the correspondence analysis radius increases to 20, the difference in the result is not much by visual inspection.

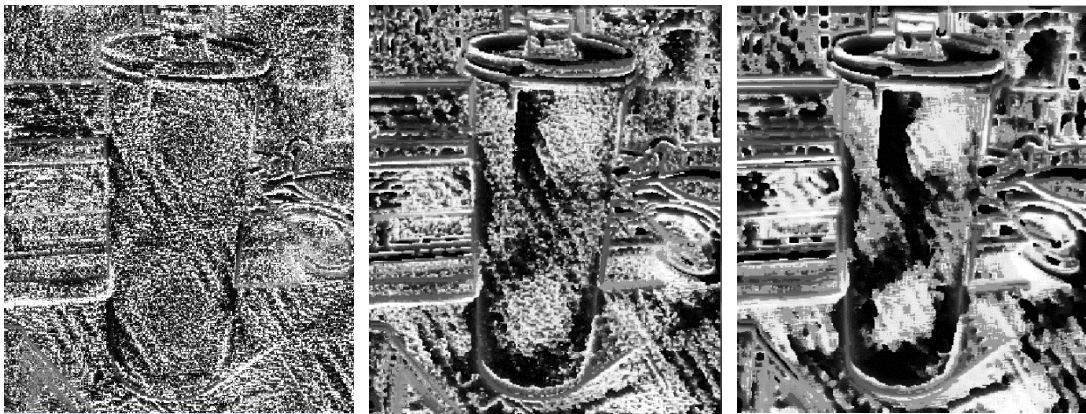


Figure 4.16: Correspondence Analysis Result – Radius = 1(Left), Radius = 9 (Middle), Radius = 20 (Right)

The effect of change in value for radius (defocus and correspondence) and the analysis result (defocus and correspondence) are tabulated in Table 4.1 and 4.2. Optimum defocus and correspondence analysis radius is needed to generate a depth representation with clear object outlines and clear distinctive features. From the tables, it can be deduced that the optimum defocus analysis radius is 1 and the optimum correspondence analysis radius is 9 to 20. Through experimental results, as the correspondence analysis radius increases above 20 the brightness of the image increases as well, but only minimal changes in clarity. Further works can be done on the outcome of this project to determine the accurate volume of the object studied for volume reconstruction purposes [12]. One of the methods for volume reconstruction can be to construct a 3D depth map using multiple cameras or using multiple view points from the object.

Table 4.1: Effect of Change in Defocus Radius on Analysis Result

	Value of Parameter	Analysis Result	
		Outline of Objects	Distinctive Features of Objects
Defocus Analysis Radius	≤ 9	As the defocus analysis radius decreases from 9 to 1, outlines of objects at different depths can be easily distinguished through observation.	As the defocus analysis radius decreases from 9 to 1, distinctive features such as cap of bottle can be seen clearly.
	> 9	As the defocus analysis radius increases from 9 to 20, outlines of objects at different depths are not able to be distinguished clearly.	As the defocus analysis radius increases from 9 to 20, there is no clear representation on distinctive features of object studied.
Conclusion	Depth representation of defocus analysis result improves as the radius decreases from 9 to 1, as the radius increases from 9 and above, the outlines and distinctive features of objects of object at different depths are not able to be distinguished clearly.		

Table 4.2: Effect of Change in Correspondence Radius on Analysis Result

	Value of Parameter	Analysis Result	
		Outline of Objects	Distinctive Features of Objects
Correspondence Analysis Radius	< 9	As the correspondence analysis radius decreases from 9 to 1, outlines of objects at different depths became more difficult to be distinguished.	As the correspondence analysis radius decreases from 9 to 1, the distinctive features of the objects became less obvious.
	≥ 9	As the the correspondence analysis radius increases from 9 to 20, outlines of objects at different depths are clearly distinguished. Brightness of the resulting image increases.	As the correspondence analysis radius increases from 9 to 20, distinctive features of the objects studied are obvious. Brightness of the resulting image increases.
Conclusion	Depth representation of correspondence analysis result deteriorates as the radius decreases from 9 to 1. As the radius increases from 9 to 20, the analysis results remain similar but the brightness of the resulting image increases, the outlines and distinctive features of objects of object at different depths are able to be distinguished clearly.		

CHAPTER 5

CONCLUSION AND RECOMMENDATION

5.1 Conclusion

In conclusion, the recently commercialised light-field camera is a very interesting concept not only for photography but for 3D reconstruction. The ability of light-field camera to capture 3D information of a scene, allows it to obtain depth data of the captured environment as well, which is essential for the purpose of 3D reconstruction. 3D reconstruction using Lytro light-field camera has three basic steps, data acquisition, data acquisition, manipulation and application. Data acquisition for this project is done by taking pictures and images using a Lytro light-field camera, data manipulation such as extracting and processing EPI and depth data, and finally the processed 3D data are used to construct a 3D digital model in the phase of application. The next step is to extract the 3D depth data in the form of matrix $[X, Y, Z]$ for 3D reconstruction. Due to the special file formats used by Lytro Company, it is necessary to find a suitable MATLAB Code that can read and manipulate the 3D data through hacking or other computation methods.

At the end of this project, 2D depth map can be generated from light field pictures while 3D depth maps can be generated using the computing defocus and correspondence algorithm [7]. The 3D depth map produced has identical shape and correct depth representations for objects based on the different colours in the depth map representing different depths of objects. Besides that, the effect of change in value for defocus and correspondence analysis radius were studied. From the results obtained, defocus analysis radius is recommended to be of a small value while correspondence analysis radius should in the range of 9 to 20 to have a correct and satisfactory depth representation. Any values higher than 20 for correspondence radius will still generate satisfactory results but with higher brightness of resulting image. By using optimum defocus and correspondence analysis radius, the result generated will have a clear representation on the outlines of objects at different depths with object's distinctive features. Therefore, the objective of this project is

achieved, which is to improve the accuracy of a 3D model reconstructed based on light-field camera by optimising the image processing steps.

5.1 Recommendation

For recommendations for this project in the future, firstly the computing depth and correspondence algorithm has to be explored more to understand the scale for scaling down the depth distance, and implement any calibration needed to obtain the real depth values. After that, the volume of the 3D depth map can be determined for future volume reconstruction purposes. Besides that, another recommendation is to make the steps to do 3D reconstruction as short and concise as possible. It is recommended to have fewer steps to achieve a satisfactory representation of 3D digital model, such as to combine the shearing EPI algorithm and the computing defocus and correspondence algorithm to save time and effort in processing the images. Another recommendation would be to use the second version of light-field camera called Illum that promises better specifications such as higher resolution of photo taken. Last but not least, it is also recommended to use softwares such as Rapidform to do 3D data management, which is powerful and robust enough to manage 3D data. Using the softwares, 3D data management such as filtering, triangulation and meshing can be done more robustly.

REFERENCE

- [1] L. Gomes, O. Regina Pereira Bellon, and L. Silva, "3D reconstruction methods for digital preservation of cultural heritage: A survey," *Pattern Recognition Letters*, vol. 50, pp. 3-14, 12/1/ 2014.
- [2] A. Koutsoudis, B. Vidmar, G. Ioannakis, F. Arnaoutoglou, G. Pavlidis, and C. Chamzas, "Multi-image 3D reconstruction data evaluation," *Journal of Cultural Heritage*, vol. 15, pp. 73-79, 2014.
- [3] J. C. Yang, M. Everett, C. Buehler, and L. McMillan, "A real-time distributed light field camera," in *Proceedings of the 13th Eurographics workshop on Rendering*, 2002, pp. 77-86.
- [4] H. Niemann and I. Scholz, "Evaluating the quality of light fields computed from hand-held camera images," *Pattern Recognition Letters*, vol. 26, pp. 239-249, 2// 2005.
- [5] A. Gallo, M. Muzzupappa, and F. Bruno, "3D reconstruction of small sized objects from a sequence of multi-focused images," *Journal of Cultural Heritage*, vol. 15, pp. 173-182, 3// 2014.
- [6] D. Reddy, J. Bai, and R. Ramamoorthi, "External mask based depth and light field camera," in *Computer Vision Workshops (ICCVW), 2013 IEEE International Conference on*, 2013, pp. 37-44.
- [7] M. Tao, S. Hadap, J. Malik, and R. Ramamoorthi, "Depth from Combining Defocus and Correspondence Using Light-Field Cameras," 2013.
- [8] D. Cho, M. Lee, S. Kim, and Y.-W. Tai, "Modeling the calibration pipeline of the Lytro camera for high quality light-field image reconstruction," in *Computer Vision (ICCV), 2013 IEEE International Conference on*, 2013, pp. 3280-3287.
- [9] T. Georgiev and A. Lumsdaine, "Depth of field in plenoptic cameras," in *Proc. Eurographics*, 2009.
- [10] P. Orchard, 'Markov Random Field Optimisation', *Homepages.inf.ed.ac.uk*, 2015. [Online]. Available: http://homepages.inf.ed.ac.uk/rbf/CVonline/LOCAL_COPIES/AV0809/ORC_HARD/. [Accessed: 24- Feb- 2015].

- [11] Optics.miloush.net, 'the file format – LYTRO meltdown', 2015. [Online]. Available: <http://optics.miloush.net/lytro/TheFileFormat.aspx>. [Accessed: 19-Feb- 2015].
- [12] W. Lu, K. Wan and J. Neiman, '3D and Image Stitching With the Lytro Light-Field Camera', 2013.